

15 Physical Systems Biology and non-equilibrium Soft Matter

C.M. Aegerter, D. Assmann (since September 2009), G. Ghilmetti (since October 2009), U. Nienhaus (since April 2009), T. Schluck, I.M. Vellekoop (till November 2009)

in collaboration with: Institute of Molecular Life Sciences (K. Basler, T. Aegerter-Wilmsen, C. Lehner, S. Luschnig), ETH Zürich (E. Hafen, I. Sbalzarini, P. Koumoutsakos), EPF Lausanne (P. Renaud, D. Floreano), University of Lausanne (S. Bergmann), Biozentrum Basel (M. Affolter), University of Strasbourg (N. Rivier), University of Konstanz (G. Maret, W. Bühner, S. Fiebig, N. Isert, C.C. Maass), Deutsches Luft- und Raumfahrtzentrum (M. Sperl), University of Twente (A. Mosk), Université Joseph Fourier Grenoble (S. Skipetrov, F. Graner), Technion Haifa (E. Akkermans), University of Exeter (P. Vukusic), Yale University (A. Monteiro).

Work in the group of physical systems biology and non-equilibrium soft-matter is concerned with the study of developmental biology using physical techniques. In this, we are developing novel imaging techniques for in-vivo imaging in turbid environments, as well as studying the influence of mechanical stresses on developmental processes. In the last year, we have made considerable progress in the development of imaging tools for turbid samples as well as the implication of mechanical forces in growth control in the wing imaginal disc of *Drosophila*.

In the imaging project, we are using wave-front shaping and the optical memory effect to create a scannable focus behind a turbid screen. Raster-scanning this focus we have then implemented into a form of fluorescence microscopy based on the use of scattered light rather than ballistic light. The long term goal of this project is to use this method in turbid situations, such as in an egg or fly pupa, where developmental processes happen hidden from view.

On the problem of the influence of mechanical forces on growth control, we have extended our modeling and experimental approach. In order to check for the possibility of mechanical stress dependent growth rates, we have simulated the tissue topology in a cellular model. This would be necessary to

create a growth control via mechanical feedback. From these simulations, we determine the neighbour distributions of the cells, as well as of the cells, which are dividing. These are then compared to experimental data, where the tissue topology is obtained from a fluorescently marked protein in the cell boundaries. While simulations without a mechanical growth stimulation contradict the data, those including mechanical feedback give excellent agreement.

15.1 Imaging through turbid media

Turbid media abound in nature. This is a major limitation in biological investigations, since direct access to the system of interest is rendered unavailable. Thus much effort has been put into increasing the depth resolution of current microscopes, with the most notable examples of confocal microscopy and two-photon fluorescence microscopy (1). However, in the case of turbid samples, even these techniques are no longer able to produce useful images, since they rely on filtering the ballistic light from a multiply scattered background. In our investigations, we use the opposite approach and control the scattered light in such a way as to produce a scannable focus. This forms the basis of a fluorescence microscope. When coherent light is multiply

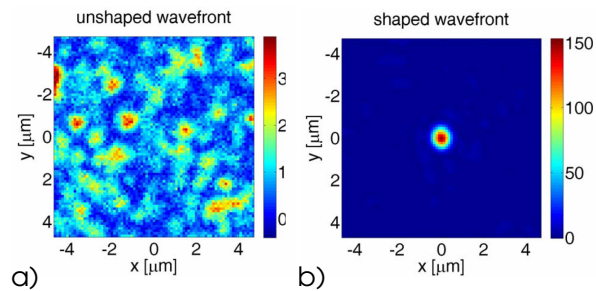


Figure 15.1: A speckle pattern (a) after illumination with coherent light onto a turbid layer. After wave-front shaping (b), the interference pattern changes to produce a narrow focus of the intensity. Note the different intensity scales on the figures. Wave-front shaping has increased the intensity of the focus more than onehundredfold.

scattered, interference on the random paths through the sample, leads to a random speckle pattern of high and low intensities. An example of this is shown in Fig. 15.1a, where the intensity behind a multiple scattering layer is shown. This pattern corresponds to a fingerprint of the sample as it corresponds to the distribution of photon-paths inside the sample. Adjusting the phase of the illuminating light in a spatially varying manner, it is possible to induce constructive interference at only one point, thus creating a focus behind a turbid sample. Several ways have been employed to achieve this, e.g. time-reversal (2), optical phase conjugation (3) and wave-front shaping (4). In Fig. 15.1b, such a focus is shown obtained using wave-front shaping.

The fact that such a focus can be formed has great implications for the possibility of imaging behind such turbid structures. If this focus can be scanned, a fluorescence based scanning microscopy can be envisaged, where the focus is scanned across a fluorescent structure. However, it would seem that this is impossible due to the delicate nature of the interference from path length differences in the random medium. A translation of the incoming light of more than a wave-length would for instance destroy the interferometric focus. For turbid samples it has however been shown that a

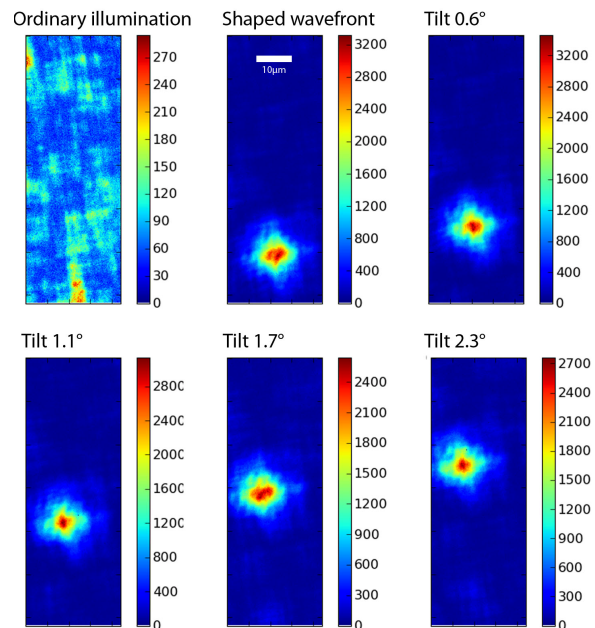


Figure 15.2: An interferometric focus behind a turbid layer is formed and then scanned over an angular range of a few degrees. This shows that it is possible to construct a scanning microscope based on interferometric focusing for samples where fluorescent structures are hidden behind turbid layers.

tilting of the wave-front leads to correlations behind the samples, which survive for small enough angles of tilt (5). The critical angle is determined by the inverse thickness of the layer and scanning over a few degrees is possible. This is shown in Fig. 15.2, where we show the position of the focus formed through a turbid layer at several stages of tilt.

Given that the interferometric focus can be scanned, we have then constructed a prototype setup, with which to demonstrate its microscope capabilities. We have used 200 nm diameter fluorescent beads, which have been added onto a cover-slip, which had a ZnO coating on the opposite side. Due to the highly scattering nature of ZnO, even a thin layer completely hides the fluorescent beads. In fact the scattering layer was such that its thickness corresponded to more than 10 mean free paths of the light. Using wave-front shaping, we have then created a fo-

cus in the plane of the fluorescent beads and scanned it over a field of view of $20 \times 20 \mu\text{m}^2$ (see Fig. 15.3 for a schematic of the setup).

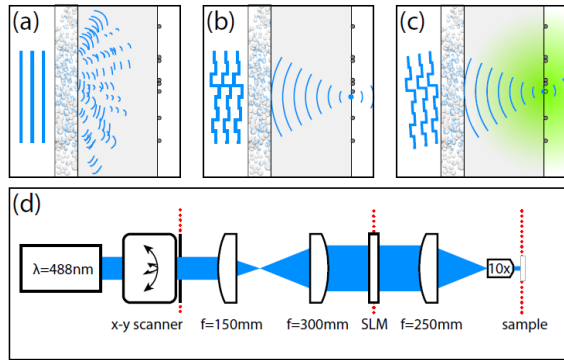


Figure 15.3: Schematic setup for the construction of a turbid microscope. A highly scattering layer of ZnO masks a collection of green fluorescent beads 200 nm in size. The thickness of the layer is more than 10 mean free paths, such that no ballistic light passes the sample. With this geometry, first an interferometric focus is formed via wave-front shaping in the plane of the fluorescent beads. This focus is then scanned using the optical memory effect and the emitted fluorescent light is collected by a photomultiplier. The scanning dependence of the intensity in the photomultiplier then corresponds to the microscopic image of the hidden structure.

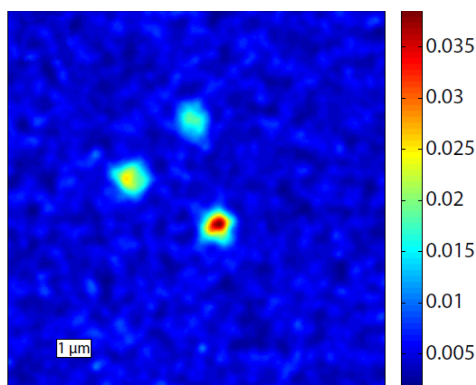


Figure 15.4: Microscopic image of three fluorescent beads behind a turbid layer more than 10 mean free paths thick. This image is obtained using the setup described in Fig. 15.3 and shows the feasibility of a scattering based microscope.

The fluorescence emitted by the beads when illuminated by the focus was collected with a photomultiplier. The dependence of this intensity in the photomultiplier on the scanning angle directly gives an scanning microscope picture of the fluorescent beads behind the turbid layer. The result of this is shown in Fig. 15.4, where a collection of three isolated beads is imaged. A cross-section of this image across a single bead, shown in Fig. 15.5, directly shows the resolution of the microscope (6). The half-width at half-maximum of the curve is at 300 nm, corresponding to the resolution. This is smaller than the wave-length of the illuminating laser used, which was 488 nm and thus can compete with high quality objectives.

Given the long term goal of applying these methods in the study of the development of *Drosophila*, we have also studied the inherent time scales in the fluctuations of the scattering medium of interest. Here, we are mainly interested in the stage of metamorphosis, where the changes to the organs occur creating them from the larval pre-cursors. This is important because the interferometric focusing relies on the stability of the turbid medium while the focus is formed (and scanned). A determination of the time scale of the fluctuations in the *Drosophila* pupa thus sets the speed needed for the imaging method. Determining the auto-correlation of a speckle behind a pupa, we found that the pattern is stable on a time scale around 10 seconds (7). This is in the range of what future developments can achieve. In fact, we have already shown that a poor focus is already possible with the current setup in a real biological specimen (7).

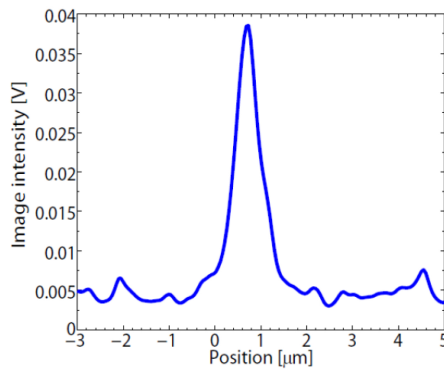


Figure 15.5: A cross-section through one of the beads in Fig. 15.4, indicating the resolution of the microscope. With a half-width at half-maximum of 300 nm, distances well below the wave-length can be resolved, competing with high quality objectives in the absence of a turbid layer.

15.2 The influence of mechanical stress on growth in the wing imaginal disc of *Drosophila*

The regulation of growth, and finally size in organs represents an interesting problem in developmental biology. One of the main subjects of study for this purpose is the wing imaginal disc of *Drosophila*. While much is known about the genetic players and growth factors, some fundamental puzzles remain. One concerns the fact that while the growth factors form spatial gradients, cell proliferation does not. We and others have recently proposed a model based on mechanical feedback that can explain this as well as the control of final size (1; 2; 3). In order to test this, we have previously studied the distribution of mechanical stresses in the tissue using photoelasticity (4). As a second step, we have now studied the possibility of feedback and a regulatory role of mechanical forces.

For this purpose, we have studied the topology of the tissue's cell shapes, which can be compared with experiments (5). Instead of describing the tissue as a fully elastic medium, our current model uses the vertices of a cellular network to describe the tissue. The mechanical properties of the tissue are then quantified by the energetics of the adhesion, surface tension and target area of the cells, which means that the positions of the vertices are obtained by minimizing an energy function first described by (6) and given by

$$\begin{aligned} E(R_i) = & \sum_{\alpha} K_{\alpha} (A_{\alpha} - A_{\alpha}^0)^2 + \\ & \sum_{(i,j)} \Lambda_{i,j} l_{i,j} + \\ & \sum_{\alpha} \Gamma_{\alpha} L_{\alpha}^2. \end{aligned} \quad (15.3)$$

Here, the index α runs over the different cells, whereas i, j describe the segments between different vertices. Moreover, K_{α} describes the area elasticity of a cell, with a preferred area A_{α}^0 , $\Lambda_{i,j}$ describes a line tension of an individual segment of length $l_{i,j}$ and Γ_{α} is a measure of the cell's contractility, leading to a min-

- [1] A. Diaspro, ed., *Confocal and Two-Photon Microscopy: Foundations, Applications and Advances* (Wiley-Liss, New York, 2002).
- [2] G. Lerosey, J. de Rosny, A. Tourin, and M. Fink, *Science* **315**, 1120–1122 (2007).
- [3] Z. Yaqoob, D. Psaltis, M. S. Feld, and C. Yang, *Nat. Photonics* **2**, 110–115 (2008).
- [4] I.M. Vellekoop and A.P. Mosk, *Opt. Lett.* **32**, 2309 (2007).
- [5] S. Feng, C. Kane, P. A. Lee, and A. D. Stone, *Phys. Rev. Lett.* **61**, 834–837 (1988); I. Freund, M. Rosenbluh, and S. Feng, *Phys. Rev. Lett.* **61**, 2328–2331 (1988).
- [6] I.M. Vellekoop and C.M. Aegerter, *Opt. Lett.* **35**, 1245 (2010).
- [7] I.M. Vellekoop and C.M. Aegerter, *SPIE proceedings* **7554**, 75420 (2010).

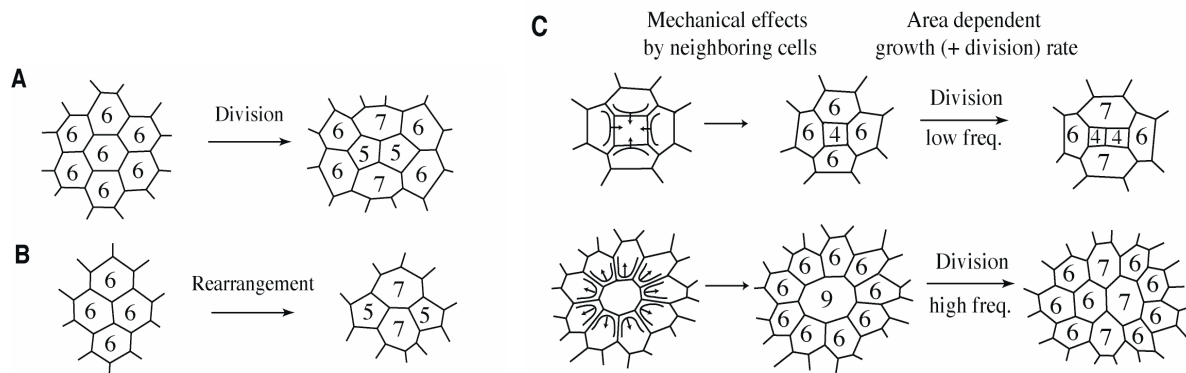


Figure 15.6: Different topological effects on a two dimensional epithelial tissue that affect the distribution of neighbour numbers. When a cell divides, the number of neighbours in the immediate surrounding of the division changes (A). This change also depends on the direction of the cell division boundary. Moreover, according to the energy function (Eq. 15.3), rearrangements of nearest neighbours are possible (T1-events, B). Finally, (C), a dependence of the division rate on the neighbour number and therefore mechanical stress will lead to an enhancement of 6 and 7-fold neighbours.

imisation of the cell's circumference L_α . This will describe the possible rearrangements depicted in Fig. 15.6B. In the simulations, all cells were treated as identical and the relative parameter values used were (6): $\Gamma/KA^0 = 0.12$ and $\Lambda/K(A^0)^{3/2} = 0.04$.

To incorporate mechanical feedback of the growth model into the topology, we have added a growth rate dependence on the number of neighbours (see Fig. 15.6C). Sub-

sequently letting cells grow, divide and rearrange according to the Hamiltonian then yields a tissue topology which is compared to the one found experimentally in Fig. 15.7. The two patterns look similar, but to quantify this, we have determined the neighbour statistics, both for all cells and for dividing (mitotic) cells only. This is shown in Fig. 15.8, where excellent agreement between the model and the experiments can be seen (7).

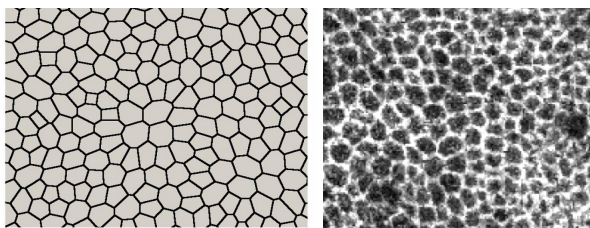


Figure 15.7: Cell shapes of a tissue both from simulation (left) and experiment (right). In the experiments, a protein present in cell membranes was fluorescently marked and imaged using confocal microscopy. From a general perspective, the two topologies look similar, which is quantitatively tested in Fig. 15.8, where the neighbour number distribution is determined.

When neglecting the possibility of rearrangements (5), both of these distributions cannot be reproduced. Not taking into account the mechanical feedback in determining the growth rates (6) does not reproduce the data for mitotic cells. This shows that mechanical stresses can play an important role in determining the tissue topology (7). Taking this together with the data on the presence of mechanical stresses (4) and the growth model (1), indicates that there is a strong role for mechanical forces in the development of the wing imaginal disc.

For future investigations, it would be ideal to have the energy terms motivated experimen-

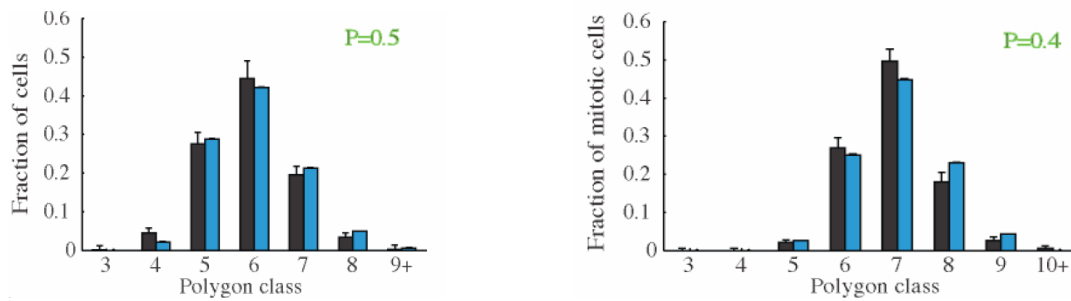


Figure 15.8: Neighbour distributions for all cells in the tissue as well as for dividing (mitotic) cells. In both cases, the simulated and experimentally determined distributions agree perfectly. When neglecting the possibility of rearrangements, the results do not agree with the experiments in both cases. Not taking into account the influence of mechanical feedback fails to reproduce the mitotic cells.

tally, which we intend to using direct mechanical stimulation of the wing disc while studying the cells. In addition, the model can also be compared directly to studies of a growing foam, since the adhesion and surface energies are known theoretically in that case.

- [1] T. Aegerter-Wilmsen, C.M. Aegerter, E. Hafen, and K. Basler, *Mech. Develop.* **124**, 318 (2007).
- [2] B.I. Shraiman, "Mechanical feedback as a possible reg-

ulator of tissue growth", *Proc. Natl. Acad. Sci. USA.* **102**, 3318 (2005).

- [3] L. Hufnagel, A.A. Teleman, H. Rouault, S.M. Cohen, and B.I. Shraiman, *Proc. Natl. Acad. Sci. USA.* **104**, 3835 (2007).
- [4] U. Nienhaus, T. Aegerter-Wilmsen, and C.M. Aegerter, *Mech. Dev.* **127**, 943 (2009).
- [5] M.C. Gibson, A.B. Patel, R. Nagpal, and N. Perrimon, *Nature* **442**, 1038 (2006).
- [6] R. Farhadifar, J.-C. Röper, B. Aigouy, S. Eaton, and F. Jülicher, *Curr. Biology* **17**, 2095 (2007).
- [7] T. Aegerter-Wilmsen, A. Christen, E. Hafen, C.M. Aegerter, and K. Basler, *Development* **137**, 499 (2010).